Understanding Friction and Wear Mechanisms of High-Purity Titanium against Steel in Liquid Nitrogen Temperature

BIKRAMJIT BASU, J. SARKAR, and RAVI MISHRA

Although the friction and wear properties of several metallic alloys in unlubricated conditions are widely investigated, such understanding for high-purity metals in cryogenic environment is rather limited. This article reports the tribological properties of high-purity α-titanium (α-Ti), prepared by cold rolling and recrystallization annealing, under liquid nitrogen (LN2) and room temperature (RT) environments against steel (bearing grade: SAE 52100) at varying loads (up to 15 N) and sliding speeds (0.6 to 4.19 m/s). It has been found that the steady-state coefficient of friction (COF) of titanium under LN2 environment (~0.27 to 0.33) is lower than that at RT COF (~0.33 to 0.58) irrespective of sliding speed. For cryogenic sliding conditions, the COF decreased steadily with sliding speed to a mean value of about 0.28 and no appreciable variation in COF is noticed for sliding speed of more than 1.5 m/s. The wear rate under both environment conditions was of the order of 10^{-3} mm^3 N^{-1} m^{-1} irrespective of variation in operating parameters, but the RT wear rate was found to be higher compared to the LN2 case. Overall, the experimental results demonstrate improved tribological properties of high-purity titanium at LN2 temperature compared to the RT. Flow localization at tribological interfaces because of the large strain rate and subsequent damage accumulation at the titanium test piece are some of the attributes of the wear of Ti at LN2 temperature. In addition, the galling of titanium was also observed to occur under large contact stress and sliding speed conditions.

© The Minerals, Metals & Materials Society and ASM International 2008

I. INTRODUCTION

AMONG the various transition metals, hexagonal closed-packed (hcp) α-titanium (α-Ti) is known to have a favorable combination of physical and mechanical properties, such as lower density (~4.5 g cm^{-3}), high melting temperature (~1668 °C), high strength, good fatigue resistance, and superior corrosion resistance.[1–4] Such attributes are responsible for the perpetual increase in the applications of titanium and its alloys in various fields such as aerospace industry, chemical industry, power engineering, construction of environment protection devices, biomedical devices, steam turbine blades, and other marine applications. In some of these applications, friction and wear of Ti is important.

However, a survey of the available open literature reveals that there are very few reports on the friction and wear behavior of high-purity titanium.[5–10] From limited results on the tribological properties of Ti-based materials, it can be inferred that, in spite of the superior combination of properties, the relatively modest hardness of Ti (H_v ~ 1 GPa), especially as compared to the widely used hardened steel (H_v ~ 7 GPa), restricts its use in heavy duty wear applications. For example, it has

been observed that ultrafine-grained titanium that has high hardness exhibits superior wear resistance than its coarse-grained counterparts during dry sliding wear against steel counterbody.[5] Efforts have also been directed toward increasing the wear resistance of titanium without compromising other specific properties. One such method includes high-temperature oxidation of titanium resulting in a significant rise of hardness due to the formation of a surface oxidized layer.[6–9] The oxide layer is found to possess superior tribological properties, *i.e.*, improved friction characteristics and low wear rate.[6,7] Additionally, Krol *et al.*[8,9] performed a comparative study of the friction and wear properties of titanium and oxidized titanium in dry sliding condition against hardened carbon steel (C45 grade). It was noted that as compared to titanium/C45 steel couple, the wear performance of the oxidized titanium/C45 couple was markedly superior.

In addition to the wear resistance, the specific strength (ratio of the strength to density) is another important engineering property that is considered for assessing suitability of an engineering material to be used in structures and also in moving parts. Titanium and its alloys are known to have better specific strength than many engineering alloys. The present study is an attempt to understand the friction and wear properties of high-purity titanium at room temperature (RT) and liquid nitrogen (LN2) temperature. This study is a part of our ongoing research in the area of cryogenic wear of materials, which has relevance to space shuttle applications.[11,12] Our recent sliding wear studies on "self-mated" stainless steel (AISI 304) and self-mated alumina

BIKRAMJIT BASU, Associate Professor, and RAVI MISHRA, Undergraduate Student, are with Laboratory for Advanced Ceramics, Department of Materials and Metallurgical Engineering, Indian Institute of Technology, IIT-Kanpur 208016, India. Contact e-mail: bikram@iitk.ac.in J. SARKAR, Sr. R&D Engineer, is with Praxair Electronics, Orangeburg, New York, NY 10962.

at LN2 temperature have exhibited lower coefficient of friction (COF, 0.1 to 0.2), yet severe wear, of the order of 10^{-4} mm^3/Nm in steel and 10^{-5} mm^3/Nm in alumina.[13,14] The term self-mated wear describes a situation in which both the mating solids, *i.e.*, the sample and the counterbody, have similar chemical composition. Low hardness of high-purity titanium at RT increases at subzero temperatures and as a consequence high-purity titanium is expected to exhibit improved tribological performance at subzero temperatures.[15] The change in deformation mode, from dislocation slip at RT to twinning at 77 K, is believed to the cause of such behavior.[15,16] In case of 3M grade Ti (unknown composition), Ostrovskaya *et al.* observed that decrease in the test temperature from 293 to 120 K resulted in a shift in the mild wear regime toward higher sliding wear.[10]

In the described backdrop, we report here our results of wear tests conducted on high-purity titanium at LN2 temperature (−196 °C). The cryogenic wear tests have been performed under varying sliding speeds (0.6 to 4.19 m/s) at a load of 10 N. The effect of load variation (5 to 15 N) at a sliding speed of 1.1 m/s has also been investigated. The sliding wear test results obtained in cryogenic test conditions have also been compared with the results of a limited number of RT tests on titanium samples.

II. EXPERIMENTAL PROCEDURE

A. *Material*

In the present investigation, high-purity hcp α-Ti disks were made to slide against steel (bearing grade) counterbody. The composition of the α-Ti has been given in Table I. The titanium discs were prepared from a 5-mm-thick plate (8 × 20 cm), which was produced by cold rolling (62 pct reduction in thickness) and then subjected to recrystallization annealing treatment at 550 °C for 5 hours. A representative optical micrograph of the polished and etched surface is shown in Figure 1. The recrystallized microstructure showed equiaxed grain structure with an average grain size of ~17 μm. These titanium samples exhibited a Vickers hardness of H_{V5} ~ 4 GPa. Spherical steel balls (bearing grade: SAE 52100) of 10-mm diameter and hardness of ~7 GPa were used as the counterbody material.

In order to estimate the hardness increase in titanium because of the reduced temperature, Rockwell hardness measurements were carried out at RT and at LN2 temperature (−196 °C). Rockwell B scale (R_B) was chosen for these measurements and the average values of at least five readings are reported here. Prior to hardness measurements at LN2 temperature, titanium
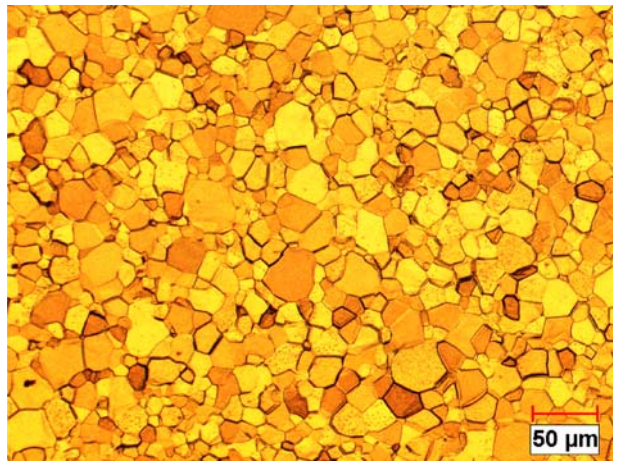
Table I. Chemical Composition of High-Purity α-Titanium*

O	C	N	Fe	S	Ti
161	27	7	5.67	3	balance

*Note: Values are in parts per million by weight (ppmw); other elements are less than 1.00 ppmw.

Fig. 1—Optical micrograph of polished and etched surface of recrystallized α-Ti, which is used as disc specimen in the present investigation.

samples were immersed in LN2 bath for approximately 90 minutes. The time gap between removal of the sample out of the LN2 bath and the hardness measurement was less than 5 seconds. The RT hardness of titanium increased from 54 R_B to 65 R_B on cooling at LN2 temperature.

B. *Wear Tests*

The sliding wear tests of high-purity α-Ti against bearing steel were performed on a high-speed ball-on-disk type cryotribometer (DUCOM, Bangalore, India), capable of operating under LN2 environment. Sliding took place between a rotating titanium disk and a stationary bearing steel ball. Figure 2 shows a schematic line diagram of the various components of the cryotribometer used in this study. The major components of this equipment include spindle assembly unit, (Figure 2(b)) specimen housing with ball-pot assembly and bearing-mounting unit, mounting arrangement of test specimen and loading arrangement, disc holder (Figure 2(c)), drive motor-gear box assembly, data-acquisition system, and electronic controller. More detailed description of the equipment can be found elsewhere.[13] The tangential friction force along with normal load and speed can be simultaneously monitored during the test using commercial software Winducom (Ducom, Bangalore, India). This equipment has been used recently for studying the cryotribological response of some of the potential structural ceramics such as Al_2O_3 and ZrO_2 and the results were reported elsewhere.[13,14]

Prior to wear experiments, both flat and ball samples were ultrasonically treated to obtain clean surfaces. The load was applied to the ball, which was held stationary in the brass ring. The brass ring was placed in a specially designed ball holder and mated against the disk rotating at the desired sliding speed. For the cryogenic wear tests, the ball/disk assembly was immersed in the LN2 and waited until all bubbles disappeared. The wear tests were carried out between 0.6 and 4.19 m/s and at a load of 10 N. The effect of load variation (5 to 15 N) on the
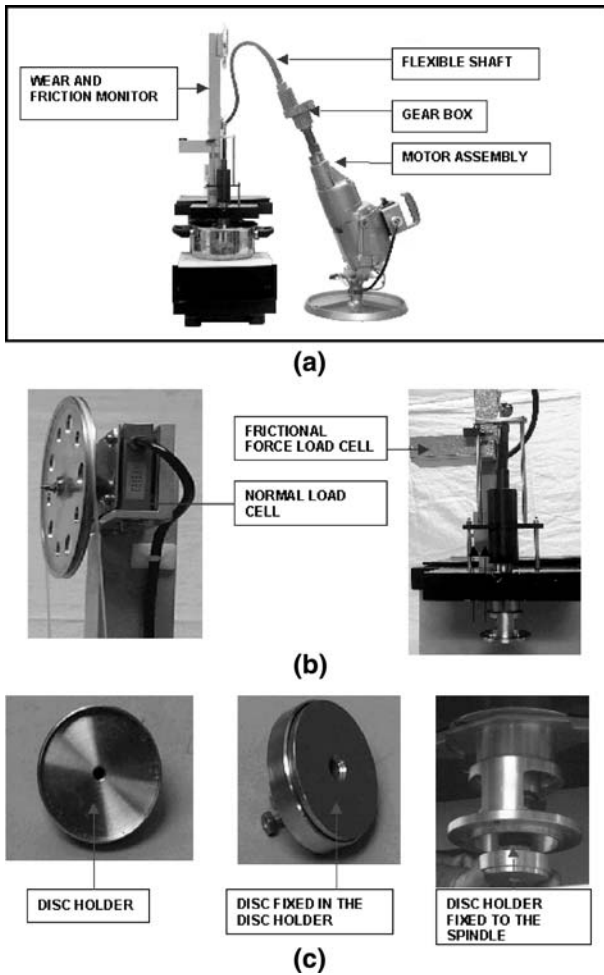
(a)

(b)

(c)

Fig. 2—(a) Schematic illustration of the entire setup of the cryogenic tribometer used in the present investigation; (b) use of dead weight during experiment as well as frictional force transducer; and (c) disc holder, which holds Ti disc against a fixed spindle during the experiment.

tribological behavior of titanium was also studied at a sliding speed of 1.1 m/s. The results of wear tests at LN2 temperatures have also been compared with the results obtained from a limited number of RT tests.

The linear sliding speed (V), corresponding to the rotational speed (rpm), is calculated as follows:

$$V \, (\text{m/s}) = 2\pi \times \text{track radius (m)} \\ \times \text{rotational speed (rpm)}/60$$

All wear experiments have been carried out at least three times to check the reproducibility of the data. In order to understand the wear mechanisms and to determine the track widths, detailed microstructural characterization of the as-worn surfaces was conducted using scanning electron microscopy–energy dispersive spectroscopy (SEM-EDS, FEI Quanta 200, Eindhoven, Netherlands). Surface profiles of the worn surfaces were acquired using laser surface profilometer to measure the depth of the wear tracks on the titanium disk. The wear track width and depth have been further used in computing the wear volume (and subsequently
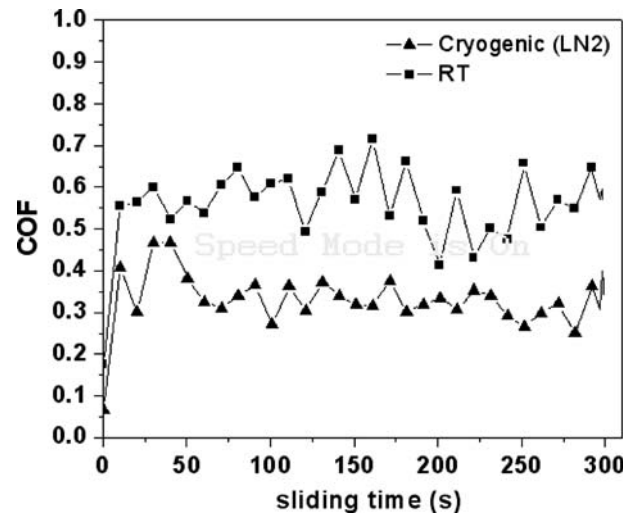

Fig. 3—Comparison of frictional behavior of α-Ti/steel tribocouple between LN2 and RT environments at a sliding speed of 0.89 ms^{-1} under 10 N load.

wear rate), which is given by the following relationships:

$$V_d \, (\text{mm}^3) = 2\pi \times \text{track radius} \times \text{track width} \\ \times \text{wear depth}$$

Wear rate (mm^3/Nm)
= worn volume/(normal load × sliding distance)

III. RESULTS

A. Friction and Wear Results

In Figure 3, representative plots show the variation of COF with sliding time in different test conditions (RT and LN2). A careful examination of the COF data reveals that the RT sliding causes greater fluctuations in COF data than in LN2 case. It needs to be mentioned here that the amplitude of such fluctuations in friction curve for RT tests increases with an increase in the sliding speed. As a result, RT sliding tests at a sliding speed greater than 1.5 ms^{-1} failed to produce steady state and tests at sliding speeds higher than this value were not conducted. It was noted that the steady-state behavior was reached within a few seconds after the tests were started. This behavior was common for sliding wear tests of dissimilar tribocouple. In Figure 4 (a), the steady-state COF data that correspond to the RT and LN2 tests are plotted against sliding speed. These results can be summarized as follows: (a) at sliding speed lower than 1.5 ms^{-1}, clearly the COF values for RT tests are higher than the LN2 tests; and (b) above 1.5 ms^{-1} sliding speed, the COF values for LN2 tests seem to stabilize to a mean value of 0.27.

Both the area and depth of the sliding wear tracks at different locations were measured by acquiring a number of two-dimensional (2-D) scans using laser
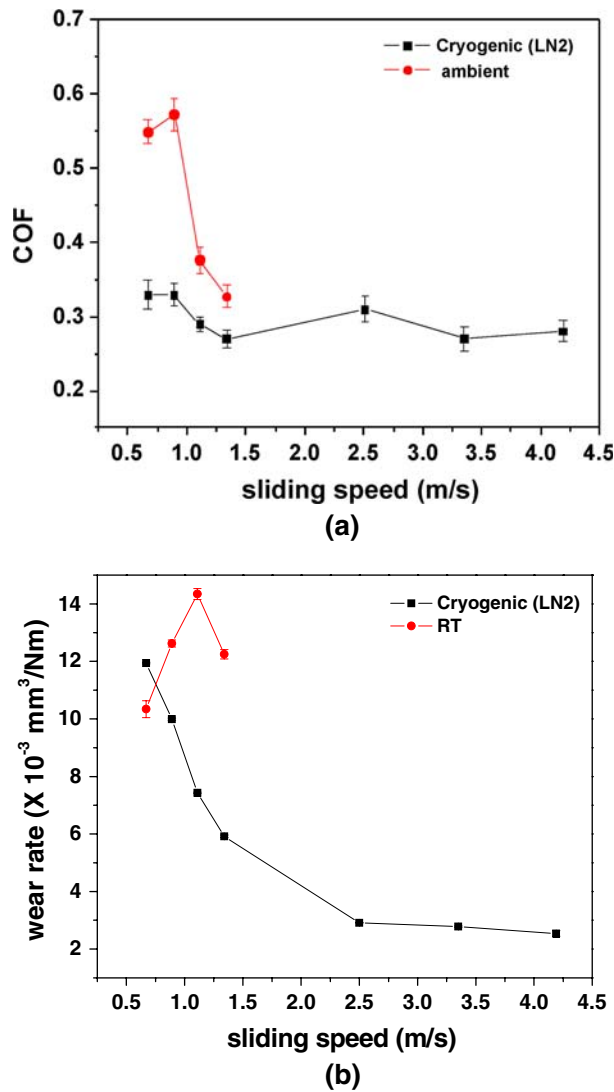
(a)

(b)

Fig. 4—Plots showing (*a*) variation of steady-state COF and (*b*) wear rate for high-purity α-Ti/steel tribocouple with sliding speed. Data correspond to 10 N load and different environments (LN2 and ambient conditions).
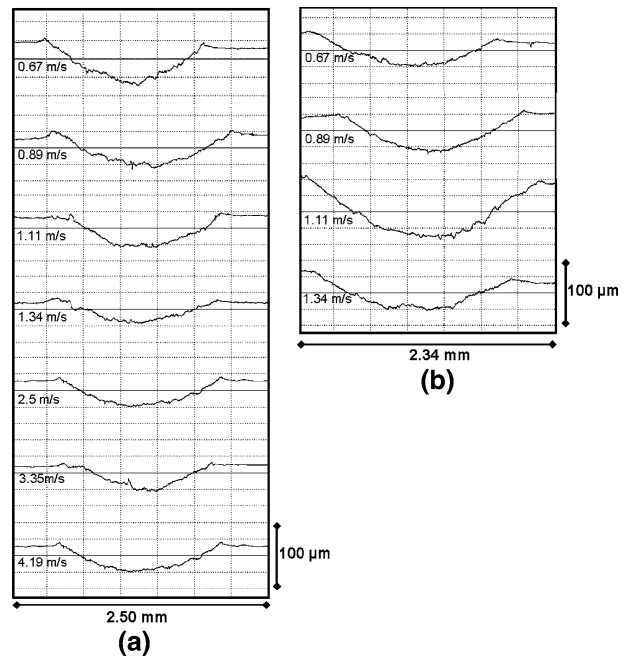

(b)

(a)

Fig. 5—2-D surface profiles of worn tracks on titanium samples after sliding tests at a normal load of 10 N. (*a*) Wear track profiles at various sliding speeds (0.67, 0.89, 1.11, 1.34, 2.5, 3.35, and 4.19 m/s) generated in LN2 tests. (*b*) Wear track profiles at various sliding speeds (0.67, 0.89, 1.11, and 1.34 m/s) generated in ambient tests. These surface profiles were recorded using laser surface profilometry.

B. *SEM-EDS Analysis of Worn Surfaces*

After the sliding tests, the detailed topographical examinations were carried out using SEM-EDS and representative SEM images are shown in Figures 6 and 7. After cryogenic testing at 10 N load, the wear tracks show mechanically damaged tribolayers (Figures 6(a) and (b)). This feature is characteristic of worn surfaces generated at various sliding speeds. At certain locations, these layers were found to be delaminated and in most cases these locations were near the center of the wear track. Figure 6(b) reveals that the damaged tribolayers are adherent to worn surface. At a sliding speed as high as 4.19 ms^{-1}, occasional delamination of the tribolayer is seen (Figure 6c). The inset of Figure 6(c) also shows some signature of the plastic flow of titanium underneath the damaged tribolayers. These are manifested in the form of elongated cavities. In addition to the abrasive wear grooves and elongated cavities, Figure 6(d) also shows some additional features, such as the formation of micron-sized spherical wear debris in the form of particles. The EDS analysis reveals that these spherical particles are predominantly Ti-oxides. These particles were found only in the pockets and did not seem to be abundant on the worn surfaces.

The characteristics of surface topography after RT sliding tests at 10 N load under varying sliding speed are shown in Figures 7(a) through (c). At a sliding speed of 0.67 ms^{-1}, the presence of deep and relatively smooth abrasive grooves on the wear track is noted (Figure 7(a)). With an increase in the sliding speed to

profilometer. Some representative 2-D profiles are shown in Figure 5 that demonstrates the severity of wear at various sliding conditions. For a given wear track the area of several such 2-D profiles were computed and the wear rate data was calculated. The measured wear rate is plotted against sliding speed in Figure 4(b). The error bars indicate the deviation of the wear rate data from their mean values. The following trends are seen. (a) For RT wear tests, although the mean wear rate seems to increase with the sliding speed, it probably remains inconclusive considering the scatter in the data. (b) In contrast to the RT tests, LN2 tests show a clear trend of systematic decrease in the mean wear rate with increasing sliding speed. (c) The difference in the mean wear rate between the RT and LN2 tests is the largest between 1.11 and 1.34 ms^{-1} sliding speed. It is also worth noting that the error bars for LN2 case are fairly tight as compared to the RT case.
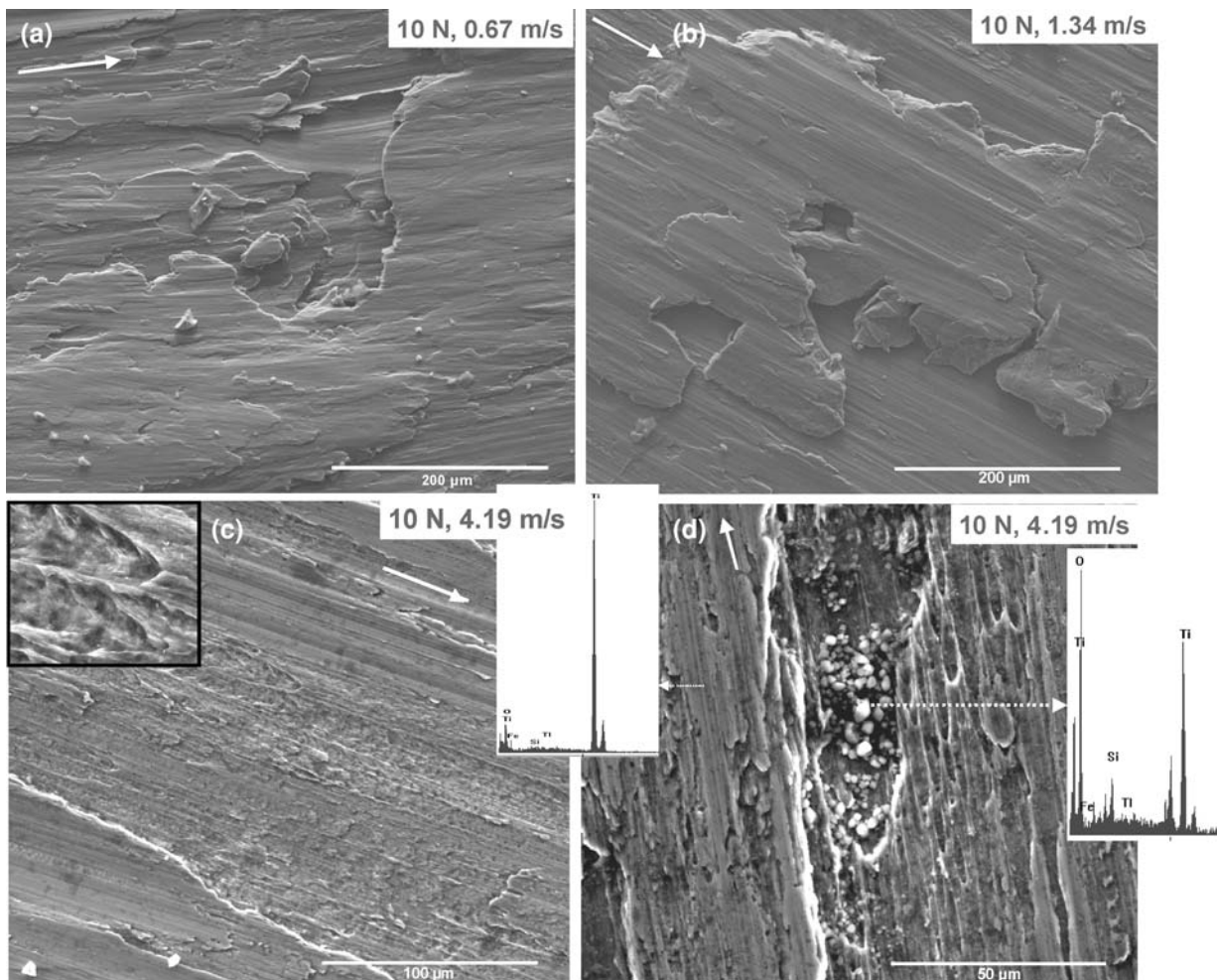
Fig. 6—SEM images showing the topographical characteristics of the wear tracks in high-purity α-Ti after sliding tests in LN2 environment. Operating conditions, *i.e.*, load and sliding speed, are mentioned against each SEM image. Details of the worn surface are shown as inset in (*c*). EDS compositional analysis of tribolayers and wear debris (spherical particles) are provided in the inset of (*d*).

more than 1 ms^{-1}, rather rough and wavy surfaces are observed (Figure 7(b)). The presence of microcracks is also visible in this test condition. At a sliding speed of 1.34 ms^{-1}, the delamination of tribolayers and severe damage to the worn surface is recorded (Figure 7(c)). In essence, RT tests generated surfaces that showed a transition from relatively smooth to damaged tribolayers with an increase in the sliding speed.

In order to study the wear characteristics of counterbody, SEM-EDS analysis of one of the steel balls was carried out and results are shown in Figure 7(d). The entire worn surface of the steel ball was found to be covered with an adherent Ti-rich tribolayer. The presence of titanium on the steel ball confirms the material transfer from the titanium test piece to the steel ball during the sliding at LN2 temperature. It is worth noting that no iron peak was recorded in multiple EDS analyses of the titanium worn surfaces at various spots. This suggests that no iron transfer took place from the steel ball to the titanium test piece. This can be rationalized by the fact that since bearing steel counterbody is harder than the titanium samples, titanium

transfer to the steel ball rather than the *vice versa* is a more likely phenomenon that can take place. Such behavior has been reported in case of mating couple made of ductile metals.[17]

IV. DISCUSSION

Titanium is one of the reactive engineering materials and prone to form titanium oxide layers even under moderate sliding conditions. Recent wear studies on titanium have shown that TiO_2 can easily be formed in dry sliding tests and the ease of formation of TiO_2 as a function of test temperature can influence the friction behavior of titanium.[5] It has been argued that the development of thick TiO_2 layer can increase the friction coefficient and can stabilize the friction behavior. It is easy to visualize that the severity of sliding condition, including the environment and the characteristics of the counterbody, would also have effects on the overall friction and wear behavior of titanium. An earlier study has shown that in atmospheric condition the friction
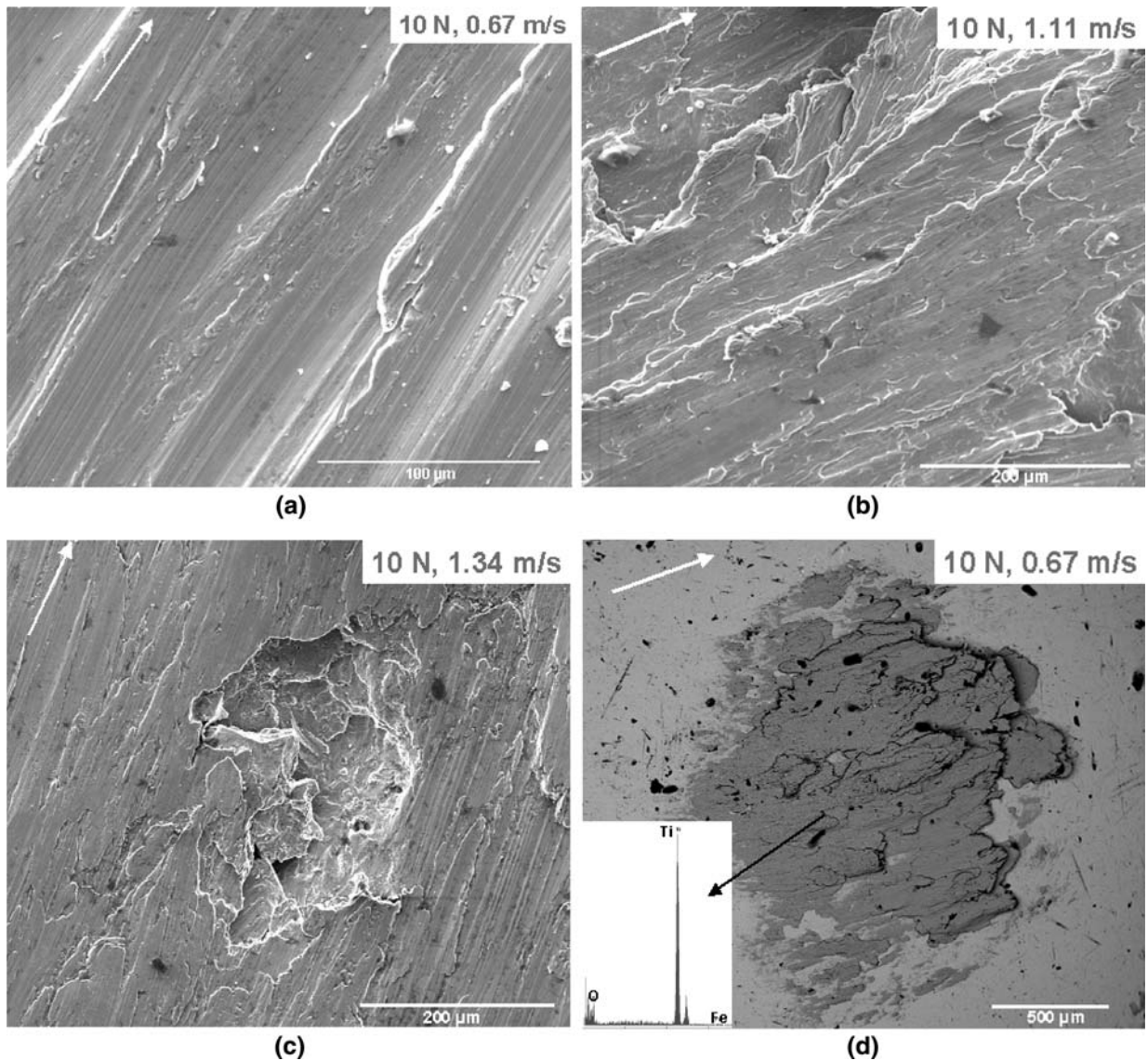
Fig. 7—(a) through (c) SEM images showing topographical characteristics of wear tracks in high-purity α-Ti after sliding tests in ambient environment. Operating conditions, *i.e.*, load and sliding speed, are mentioned against each SEM image. (d) SEM image showing characteristics of worn surface of the counterbody (bearing steel ball). EDS compositional analysis of the tribolayer is shown in inset of (d).

surface temperature can easily reach several hundred degrees Celsius and form TiO_2 layers.[5] However, when a cryogenic liquid is used as an environment, as in this case, there would be various influencing factors such as quenching of the friction surface temperature, blanketing of oxygen flow from the atmosphere to the friction surface, perhaps a degree of lubrication from the cryogenic liquid itself, and also hardening of the test material and counterbody. In case of liquid nitrogen, the boiling point is −196 °C and it is believed that the friction surface temperature (reflected in the flash temperature) can to some extent be reduced by rapid heat extraction from the friction surfaces. The reduced test temperature also increases the hardness of the titanium test piece by 10 units of R_B as well as the counterbody. In this backdrop, the present study addresses the following questions: (a) whether LN2 can influence frictional behavior to any noticeable

extent, (b) whether the sliding tests in LN2 temperature influence the wear rate of titanium as compared to the RT sliding tests, and (c) whether deformation or fracture at subzero temperature contributes to the sliding wear properties of Ti/steel tribosystems. The wear test data as a function of test variables and the wear surface characteristics essentially have components of the controlling factors that have been discussed previously. In assessing the issues, two broad aspects, one based on flash temperature at the tribocontact and the other based on the stress-assisted deformation, will be discussed subsequently.

A. *Thermal Aspect*

From a phenomenological point of view, high sliding speed causes an increase in the contact temperature (flash temperature), which often helps oxidation

reaction to take place. Therefore, the flash temperature sheds some degree of light on the overall wear mechanisms at various test conditions. Since the flash temperature has not been experimentally measured in the present study, the following established formulation has been used to estimate the flash temperature:[18]

$$T_f - T_{b'} = \frac{\mu F_v}{A_r} \left(\frac{1}{\frac{k_1}{l_{1f}} + \frac{k_2}{l_{2f}}} \right) \qquad [1]$$

$$T_{b'} = T_b - \frac{A_r}{A_n} (T_b - T_0) \qquad [2]$$

$$T_b = T_0 + \frac{\mu F_v}{A_n} \left(\frac{1}{\frac{k_1}{l_{1b}} + \frac{k_2}{l_{2b}}} \right) \qquad [3]$$

where A_n is nominal contact area (m^2), A_r is real (total asperity) contact area (m^2), l_{1b} and l_{2b} are equivalent linear heat-diffusion distances for two mating surfaces (bulk heating, m), l_{1f} and l_{2f} are equivalent linear heat-diffusion distances for two mating surfaces (flash heating, m), F is normal load acting on the sliding surfaces (N), v is sliding speed (ms^{-1}), μ is COF, k_1 and k_2 are thermal conductivities of two solid counterfaces (W/m/K), T_0 is heat sink (ambient) temperature (K), T_b is bulk temperature (K), $T_{b'}$ is effective sink temperature for flash temperature calculation (K), and T_f is flash temperature (K).

All the basic parameters including thermal conductivity values considered in our estimation for flash temperature are mentioned in Table II. Since no experimentally measured thermal conductivity data is available for titanium at LN2 temperature (−196 °C), the available data for annealed polycrystalline titanium[19] are extrapolated to LN2 temperature. Also due to the unavailability of the thermal conductivity data of steel at subzero temperature in the open literature,[19,20] the conductivity of polycrystalline iron is considered in the present case. As will be explained in Section IV–B, the investigated tribocouple has the nominal contact radius of 77 μm and therefore, the nominal contact area (A_n) is 1.86 × 10^{-8} m^2. All other parameters such as l_{1b}, l_{2b}, l_{1f}, and l_{2f} are dependent on the operating parameters like sliding velocity. Based on Eqs. [1] through [3] and the measured COF data, the flash temperature values have

been estimated and these data are summarized in Table III. It should be noted that the bulk temperature (T_b) does not vary much with sliding speed and is taken as 25 °C for ambient tests and −196 °C for LN2 tests. From Table III, it is also clear that at any given sliding speed (<1.5 m/s), the flash temperature is noticeably higher in an ambient test than in a test conducted at LN2 temperature. For example, a flash temperature of 340 °C during ambient test condition and 76 °C during LN2 test has been predicted at sliding speed of 1.34 m/s. Interestingly, the subzero flash temperature has only been predicted for LN2 test at the lowest speed of 0.67 m/s. Although not mentioned in Table III, a maximum flash temperature of around 672 °C has been estimated at the highest sliding speed of 4.19 m/s in LN2 environment. Such high flash temperature, which could be realized at the asperity/asperity junctions under the most severe operating conditions in cryogenic conditions, however, is much lower than the temperature for phase transformation of α-Ti to bcc β-Ti. Also, high flash temperature of 369 °C and 480 °C at sliding speed of 2.51 and 3.35 m/s are estimated, respectively.

At low sliding speeds (<1.5 m/s), lower flash temperatures (<100 °C) essentially reduce the chances of extensive oxide formation in tests in LN2 environment. More importantly, LN2 environment acts as a blanket and minimizes oxygen flow to the friction surface. This would limit the oxidative reactions at the friction surface. It should be noted that at all sliding speeds in LN2 temperature test tribolayers have similar features, i.e., abrasion marks and occasional microcracks of the layers. The examination of COF data for LN2 tests reveals that the COF is largely independent of the sliding speed. This is consistent with the surface characteristics as explained previously. In addition, underneath the damaged tribolayers and in pockets, oxide and oxide-coated wear debris have been found. This applies to very high sliding speed of 4.19 m/s. It should be recalled that the boiling temperature of LN2 is −196 °C and the flash temperature at this sliding speed is 672 °C. It is very unlikely that LN2 will actually act as a blanket at this high temperature and would evaporate to allow oxygen to reach the friction surface. This indicates that the formation of oxide is possible at very high sliding speeds (e.g., 4.1 m/s) and Figure 6(d) reveals oxide debris underneath tribolayers. Since the COF of the investigated tribosystem is much higher than 0.1, the possibility of any lubricating effect from LN2 is remote. Rough worn surfaces of samples tested in LN2 (Figures 6(a) through (c)) in fact confirm the absence of lubricating effect from LN2.

Table II. Various Parameters Used in the Computation of the Flash Temperature*[17,18]

| Material | Thermal Conductivity (k, W/m/K) | | A_n (m^2) | T_0 (K) | |
	Ambient	LN2		Ambient	LN2
Ti	15	27	1.86 × 10^{-8}	298	77
Steel	71	175			

*Note: While the thermal conductivity values are obtained from Ref. 18, the nominal contact area (A_n) is measured on the basis of the Hertzian contact dimension, as described in Section IV–B.

Table III. Calculated Flash Temperatures as a Function of Sliding Wear Test Conditions

| Sliding Speed (ms^{-1}) | Normal Load (N) | T_f (°C) | | T_b (°C) | |
		Ambient	LN2	Ambient	LN2
0.67	10	251	−37	25	−196
0.89		333	14		
1.11		314	42		
1.34		340	76		

In case of RT tests, even low enough flash temperatures at slow sliding speeds can easily form TiO$_2$ layers because of the abundance of oxygen from the atmosphere and raises the COF.[5] With increasing sliding speed the softening of the counterbody (here steel ball) seems to be a dominant factor and probably brings down the COF by a large magnitude. This drop in the COF is probably larger than the rise in the COF because of the formation of TiO$_2$ layers.

As discussed previously, from low to medium sliding speeds the existence of tribolayers is clear from the micrographs taken on the worn surfaces (Figures 6(a) through (c)). It appears that in LN2 environment, titanium friction surfaces are largely able to retain the tribolayers up to fairly large sliding speeds, and the underlying metal is being prevented from further wearing. Fine microcracks and delamination of tribolayers at certain locations failed to increase the wear rate even at high sliding speeds. In case of RT tests, even at very low sliding speed such as 1.34 m/s, delamination of tribolayers is very clear (Figure 7(c)). This explains a significant increase in the wear rate in RT tests as compared to the tests conducted at LN2 temperature.

B. *Tribomechanical Stress-Assisted Deformation and Damage*

In the plane of worn surfaces, we have seen (a) the formation of tribolayers in both LN2 and RT cases because of the severe plastic deformation, (b) flow localization in the form of elongated cavities in LN2 case (Figure 6(c)), and also (c) the damage of the tribolayer in RT case (Figure 7(c)). All such topography development, in the light of the previous discussion, can be attributed to large plastic shear strains that resulted from sliding wear tests. Subsequently, an attempt will be made to estimate the magnitude of the contact stress and the contact dimension and to assess the possible influence of stress on the plastic deformation.

The contact pressure at the metal surface has been estimated by applying the concept of Hertzian contact stress field, *i.e.*, the mean (average) Hertzian contact pressure.[21]

$$P_m = (W/\pi a^2) \qquad [4]$$

The initial contact diameter (*a*) is given by[24]

$$a = (3WR/4E^*)^{1/3} \qquad [5]$$

where P_m is the mean contact pressure, W is the applied load, E^* is the effective elastic modulus, and R is the radius of the ball counterbody.

The effective elastic modulus E^* can be calculated using the following equation:[21]

$$1/E^* = (1 - v_1^2)/E_1 + (1 - v_2^2)/E_2 \qquad [6]$$

where E_1 and E_2 are the elastic modulus of the mating solids and v_1 and v_2 are the Poisson's ratio of the contacting solids.

Taking the Poisson's ratio equal to 0.3 for both titanium and the steel, elastic modulus of the steel as 210 GPa and that of titanium as 110 GPa, the mean contact stress and contact diameter at 10 N load have been estimated to be 536.7 MPa and 77 μm, respectively. Recently, Ko *et al.* compared the deformation characteristics of coarse-grain (~15 μm size) titanium with ultrafine-grain high-purity titanium produced by equal channel angular processing.[22] An ultimate tensile strength of 350 MPa and a total strain-to-fracture of 35 pct were measured for coarse-grained titanium in a RT uniaxial tensile test. Titanium used in the present study has comparable average grain size of 17 μm and it can therefore be concluded that the initial Hertzian contact stress level at the contact spots are much higher than the uniaxial tensile strength recorded in Reference 22. Often calculation of failure stresses of ductile materials using tensile loads at failure strains and the cross-sectional area of fractured surfaces lead to much higher values than the ultimate tensile strengths. Therefore, the difference between the mean contact stress and the ultimate tensile strength can perhaps be related to the development of cavity formation assisted by the shear flow localization as seen in tensile tests between the starting point of necking and the point of failure.

The initial Hertzian contact diameter (77 μm) was calculated to be approximately five times the average grain size (17 μm) of the titanium samples used in this study. However, the final wear track width was found to be at least one order of magnitude higher than the initial Hertzian contact diameter of 77 μm. This can be rationalized by the fact that initially a few grains experience Hertzian contact stress field, and with the progression of wear more grains experience deformation-induced damage. Therefore it presents a picture that a large number of real contacts or microregions of large strains are generated across a significant number of grains during the wear process.

Another experimental observation that requires explanation is the establishment of Ti/Ti contact during sliding wear tests in the present case (Figure 7). The transfer of titanium from the test piece to the steel ball and associated topographical features of surfaces confirms occurrence of "galling."[23] By definition, galling is a condition whereby excessive friction between high spots of mating parts results in localized welding with subsequent splitting and a further roughening of rubbing surfaces of one or both the mating parts. The occurrence of galling has been widely reported in case of sliding of uncoated high-purity titanium against titanium alloys in unlubricated tests.[24–27] Based on the results from a number of wear tests on uncoated titanium, Wiklund and Hutchings were able to identify the onset of galling at a load as low as 5 N.[24] In the present study, a much higher load of 10 N has been used and this might have helped galling to occur in titanium/steel tribosystem. The SEM results verify the occurrence of the galling of titanium under the given set of test conditions.

V. CONCLUSIONS

The following conclusions can be drawn from the present study on the tribological behavior of high-purity

titanium sliding against steel balls (bearing grade) in RT and LN2 environments.

1. The COF was largely independent of the sliding speed for the LN2 case, though it depended on the sliding speed in RT case. Higher COF with large fluctuation was recorded at lower sliding speeds in both types of environments. At sliding speed of lower than 1 m/s, much higher COF of 0.4 or a larger value is recorded during RT sliding, while COF varies in the narrow window of 0.25 to 0.35 in LN2 case during various sliding test conditions.
2. Wear rates were found to be of the same order $(10^{-3}$ mm^3 N^{-1} m$^{-1})$ in both environments but they were comparatively low in LN2 environment. At a sliding speed of higher than 1 m/s, the wear rate was found to be independent of the sliding speed. The wear depths of worn titanium disks varied between 32 and 58 μm.
3. Flow localization at tribological interfaces because of the large strain rat and subsequent damage accumulation at the titanium test piece are some of the attributes of the wear at LN2 temperature. In addition, the galling of titanium was also observed to occur under large contact stress and sliding speed conditions. The SEM results verify the galling of titanium on steel ball.
4. Based on the results from friction studies and worn surface characterization, it can be concluded that the effect of LN2 was pronounced in lowering the COF and the wear rate of high-purity titanium. This has been partially explained by the flash temperature at the tribocontact, which is much lower in LN2 environment than that during ambient tests. In particular, the absence of oxidative wear at lower sliding speed ($<$1.5 m/s) is attributed to lower flash temperature of less than 100 °C in LN2 environment.

ACKNOWLEDGMENTS

REFERENCES

1. B.H. Hanson: *Mater. Des.*, 1986, vol. 7, pp. 301–07.
2. H. Dong and T. Bell: *Wear*, 2000, vol. 238, pp. 131–37.
3. A. Choubey, B. Basu, and R. Balasubramaniam: *Mater. Sci. Eng.*, 2004, vol. A379, pp. 234–39.
4. A. Choubey, B. Basu, and R. Balasubramaniam: *J. Alloys Compd.*, 2004, vol. 381, pp. 288–94.
5. P.Q. La, J.Q. Ma, Y.T. Zhu, J. Yang, W.M. Liu, Q.J. Xue, and R.Z. Valiev: *Acta Mater.*, 2005, vol. 53, pp. 5167–73.
6. D.S.R. Krishna, Y.L. Brama, and Y. Sun: *Tribol. Int.*, 2006, in press.
7. P.A. Dearnley, K.L. Dahma, and H. Çimenoglu: *Wear*, 2004, vol. 256, pp. 469–79.
8. S. Krol, Z. Zalisz, and M. Hepner: *J. Mater. Process. Technol.*, 2005, vols. 164–165, pp. 868–75.
9. S. Krol, L. Ptacek, Z. Zalisz, and M. Hepner: *J. Mater. Process. Technol.*, 2004, vols. 157–158, pp. 364–69.
10. Y. Ostrovskaya, T.P. Yukhno, G.D. Gamulya, Y.V. Vvedenskij, and V.I. Kuleba: *Tribol. Int.*, 2001, vol. 34, pp. 265–76.
11. T. Gradt, T. Schneider, W. Hübner, and H. Börner: *Int. J. Hydrogen Energy*, 1998, vol. 23, p. 397.
12. R. Khanna and B. Basu: *J. Am. Ceram. Soc.*, 2007, vol. 90, pp. 2525–34.
13. B. Subramonian and B. Basu: *Mater. Sci. Eng.*, 2006, vol. A415, pp. 72–79.
14. R. Khanna and B. Basu: *J. Mater. Res.*, 2006, vol. 21, p. 831.
15. O.M. Ivasishin, P.E. Markovsky, G.A. Pakharenko, and A.V. Shevchenko: *Mater. Sci. Eng.*, 1995, vol. A196, pp. 65–70.
16. Q.Y. Sun, X.P. Song, and H.C. Gu: *Int. J. Fatigue*, 2001, vol. 23, pp. 187–91.
17. D.A. Rigney: *Wear*, 2000, vol. 245 (1), pp. 1–9.
18. H.S. Kong and M.F. Ashby: *Mater. Res. Soc. Bull.*, 1991, vol. 16 (10), pp. 41–48.
19. L.D. Marks, S.S. Perry, and W.G. Sawyer: in *Materials at Low Temperatures*, R.P. Reed and A.F. Clark, eds., ASM, Metals Park, OH, 1960.
20. H.M. Rosenberg: *Philos. Trans. R. Soc. London, Ser. Math. Phys. Sci.*, 1995, pp. 441–97.
21. B. Bhushan: *Principles and Applications of Tribology*, John Wiley & Sons, New York, NY, 1999, pp. 205–07.
22. Y.G. Ko, D.H. Shin, K.-T. Park, and C.S. Lee: *Scripta Mater.*, 2006, vol. 54, pp. 1785–89.
23. *American Society for Testing and Materials*, Standard G40-98b, Standard Terminology Relating to Wear and Erosion, ASTM, West Conshohocken, PA, 1999.
24. U. Wiklund and I.M. Hutchings: *Wear*, 2001, vol. 251, pp. 1034–41.
25. M. Long and H.J. Rack: *Wear*, 2001, vol. 249, pp. 158–68.
26. L. Vitos, K. Larsson, B. Johansson, M. Hanson, and S. Hogmark: *Comput. Mater. Sci.*, 2006, vol. 37, pp. 193–97.
27. A. Crossleya, C. Johnston, I.M. Hutchings, S. Myhra, J.A.G. Temple, and U. Wiklund: *Thin Solid Films*, 2002, vol. 414, pp. 224–30.